Space-Time Block-Coded OFDMA With Linear Precoding for Multirate Services

Anastasios Stamoulis, Zhiqiang Liu, and Georgios B. Giannakis, *Fellow, IEEE*

***Abstract*—Relying on space-time linearly precoded orthogonal frequency-division multiple access (OFDMA) and exploiting both transmit and receive antenna diversity, we design herein multirate transceivers that guarantee deterministic symbol recovery with diversity gains regardless of the (possibly unknown) frequency-selective finite impulse response (FIR) channels and multiuser interference. Our approach is based on a three-level design of user codes: the top level (based on OFDMA) handles multiuser interference, the middle level (based on space-time block coding) results in space-time diversity gains, and the lower level (based on linear precoding) mitigates intersymbol interference (ISI). In a multiuser/multirate setting, with two transmit and a single receive antenna, our designs achieve guaranteed diversity gains, whereas the use of two receive antennas could potentially double the capacity of the system (in terms of maximum number of users or achievable transmission rates) under favorable conditions (such as no frequency offset). Simulations illustrate the merits of our approach.**

***Index Terms*—Diversity, linear precoding, OFDM, space-time coding.**

I. Introduction

BROADBAND wireless networks are envisioned to provide high data rates and support integrated services. To make them possible, the physical layer should i) cope with the variable channel capacity due to multipath fading; and ii) facilitate multiuser/multirate transmissions. Time, frequency, and spatial diversity have been employed to combat channel fading and the high bit-error-rates (BERs) it induces (see, e.g., [11], [12], and references therein). Time diversity (e.g., through interleaving and channel coding) is achieved at the expense of reduced data transmission rate, frequency diversity comes at the expense of bandwidth overexpansion, and spatial diversity requires (generally) extra hardware. Among the three, spatial diversity especially with transmit antennas has drawn a lot of attention recently as it promises to increase the achievable transmission rates significantly.

On the other hand, the capability for multiuser/multirate transmissions is a prerequisite of integrated services architectures that attempt to support a number of users and applications with diverse needs in delay, throughput, and BER. One way of implementing multiuser/multirate services is by using time-division multiple access (TDMA) with an underlying code-division multiple access (CDMA) or OFDM-based physical layer; see, e.g., [26] for a theoretical framework and [3] for a practical system (such as the HiperLan 2). However, a multirate/multiuser physical layer could dispense with TDMA and offers additional advantages such as opportunities for greater frequency reuse [23] and more accurate implementation of network layer transmission schedules [17].

In this paper, we develop a novel multirate/multiuser scheme relying on space-time (ST) linearly precoded orthogonal frequency-division multiple access (OFDMA) that exploits both transmit and receive antenna diversity. The resulting transceivers rely on block-spreading to guarantee symbol recovery with diversity gains, regardless of the (possibly unknown) frequency-selective FIR channels and multiuser interference (MUI). Our approach is based on a three-level user code design.

1) The top level (based on OFDMA) handles MUI.
2) The middle level (based on space-time block coding) results in ST diversity gains.
3) The lower level (based on linear precoding) mitigates intersymbol interference (ISI).

The novelties of our work do not lie solely on the seamless integration of ideas found in space-time block coding, OFDMA, and linear precoding. We also investigate the impact of receive antenna diversity on our block-spreading codes and develop novel receive structures that capitalize on it.

The merits of block spreading with an inner/outer code design have been introduced in [6], [8], [25], and [26] for block transmission systems. The inner code can be realized either through channel coding or redundant linear precoding. The latter introduces significantly less redundancy than channel coding and may be more effective in mitigating the effects of FIR channels (see [8] and references therein). The outer code (which could take the form of time slots in TDMA or user codes in CDMA) eliminates MUI and converts multiuser environments to single-user ones. Based on subcarrier allocation, the outer code of [6], [8], [25], and [26] offers flexible rate allocation and deterministic MUI elimination, regardless of the underlying FIR channels, while adhering to a low-implementation cost (most of operations are FFT based). However, the framework of [6], [8], [25], and [26] does *not* incorporate ST coding.

ST coding capitalizes on multiple transmit antennas to increase considerably the channel capacity [5]. Although it is well known that array processing and receive antennae improve BER performance, the size-power limitations of handheld devices

Manuscript received August 24, 2000; revised October 1, 2001. This work was supported by the National Science Foundation under Wireless Initiative Grant 99-79443. The associate editor coordinating the review of this paper and approving it for publication was Dr. Vikram Krishnamurthy.

A. Stamoulis is with the AT&T Shannon Laboratory, Florham Park, NJ 07932 USA.

Z. Liu is with the Department of Electrical and Computer Engineering, University of Iowa, Iowa City IA 52242 USA.

G. B. Giannakis is with the Department of Electrical and Computer Engineering, University of Minnesota, Minneapolis, MN 55455 USA (e-mail: georgios@ece.umn.edu).

Publisher Item Identifier S 1053-587X(02)00416-6.

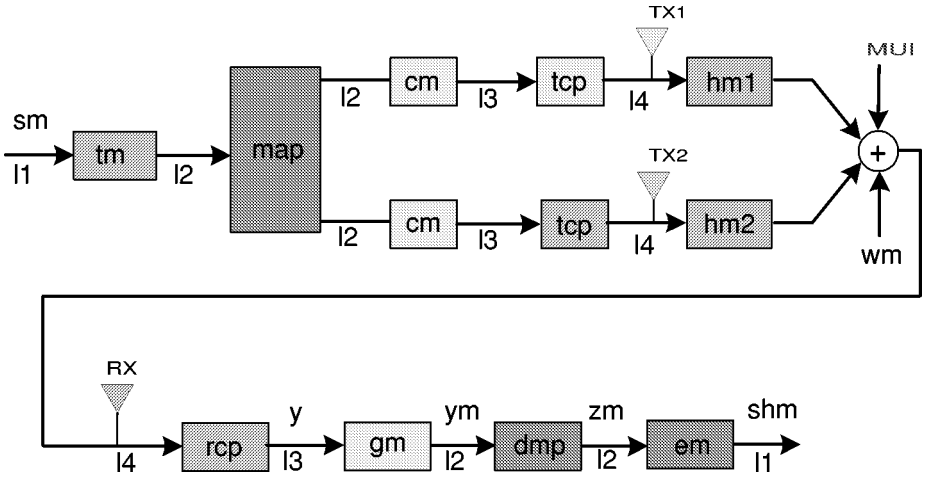

Fig. 1. Physical layer.

make the deployment of multiple transmit antennas at the basestation an attractive alternative. ST coding can achieve spatial diversity gains with just a single receive antenna; multiple receive antennas are optional (as we show in this work, if the receiver is equipped with more than one receive antenna, further performance improvement can be achieved). Systems equipped with ST coding are multi-input multi-output (MIMO) systems where serial information symbols are coded across both "space" (as the same symbols are transmitted by multiple transmit-antennas) and "time" (as the same symbols are repeated at different time slots). The received symbols are jointly decoded to recover the information symbols with diversity and coding gains. A tutorial on ST coding can be found in [11] and [12].

In broadband wireless networks, ST coding must take into consideration channel frequency-selectivity [11]. ST decoding schemes based on maximum-likelihood estimators may not be attractive, especially given the limited processing resources of handheld devices and their exponential computational complexity. Decoupling ST decoding from channel equalization appears to be a computationally attractive alternative, and it has already been proposed in the form of ST-coded OFDM [1]. However, the inner/outer code designs of [26] exhibit improved BER performance with respect to OFDM, which in part motivated the development of *single-rate* ST block codes in [10] with *a single receive antenna*.

Herein, we combine the strengths of [26] (multirate services, deterministic MUI/ISI suppression) with those of [10] (ST diversity gains in the presence of frequency-selective fading channels) while augmenting both schemes. In Section II, we incorporate the ST code of [10] into the framework of [26]. In Section III, we study how multiple receive antennas affect our block-spreading code and receiver design. Keeping in mind that receive antenna diversity can be used to separate users in space, we prove that in frequency-selective channels, while ensuring ST diversity gains and without increasing the order of the computational complexity, either transmission rates or the maximum number of active users can be doubled just by deploying a second receive antenna under favorable conditions (such as no frequency offset). The merits of our system are verified through simulations in Section IV. Finally, Section V concludes and gives pointers to future research.

II. Physical Layer

First, we provide a high-level view of our physical layer, and then, we provide a detailed mathematical description.

High-Level View: At the physical layer, there are $N_t = 2$ transmit antennas and $N_r = 1$ receive antenna for each of M users, as shown in Fig. 1. User m, $m = 0, \ldots, M-1$ relies on a block-spreading code to transmit information symbol blocks $\boldsymbol{s}_m(n)$ of size $K_m \times 1$. Through the $J_m \times K_m$ linear precoder $\boldsymbol{\Theta}_m$ $(J_m > K_m)$, the blocks $\mathbf{s}_m(n)$ are mapped to $J_m \times 1$ blocks $\tilde{\mathbf{s}}_m(n)$; the ST mapper $\mathcal{M}(\cdot)$ maps two consecutive blocks $\tilde{\mathbf{s}}_m(2n)$, $\tilde{\mathbf{s}}_m(2n+1)$ to four blocks $\bar{\mathbf{s}}_{mi}(2n)$, $\bar{\mathbf{s}}_{mi}(2n+1)$, $i = 1, 2$ (where the index i denotes the transmit antenna). The coded blocks $\bar{\mathbf{s}}_{m1}(2n)$, $\bar{\mathbf{s}}_{m1}(2n+1)$ are to be parallel-to-serial converted, pulse-shaped, and transmitted by the first antenna, and likewise, $\bar{\mathbf{s}}_{m2}(2n)$ and $\bar{\mathbf{s}}_{m2}(2n+1)$ are to be transmitted by the second antenna. The user-specific OFDMA code matrix $\mathbf{C}_m$ maps each block to a $P \times 1$ transmitted block $\mathbf{u}_{mi}(n)$, where $P = \sum_{\mu=0}^{M-1} J_\mu$. Before the transmission of $\mathbf{u}_{mi}(n)$, the last L elements of $\mathbf{u}_{mi}(n)$ are copied to its beginning to avoid inter-block interference (IBI) caused by the FIR channel.[1] This operation is represented by the matrix $\mathbf{T}_{cp}$ and implements the cyclic prefix (CP) as in OFDM. The $(P+L)$-long transmitted block goes through the FIR channel, which is denoted by the Toeplitz matrix $\mathbf{H}_{mi}$. As a result, the received block $\mathbf{y}(n)$ obtained after sampling the receive-filter output at the chip rate and discarding the CP still contains MUI and additive noise $\eta(n)$ (see Fig. 1). The retrieval of the transmitted data $\mathbf{s}_m(n)$ (of the mth user of interest) entails the following steps at the receiver:

1) elimination of MUI, which is achieved by the $J_m \times P$ receive matrix $\mathbf{G}_m$, which is applied to $\mathbf{y}(n)$ to produce the MUI-free block $\mathbf{y}_m(n) = \mathbf{G}_m \mathbf{y}(n)$;
2) linear processing of the MUI-free block $\mathbf{y}_m(n)$ by the ST decoder $\bar{\mathcal{M}}(\cdot)$ to achieve transmit diversity gain regardless of the (possibly unknown) FIR channels; $\bar{\mathcal{M}}(\cdot)$ produces $J_m \times 1$ blocks $\mathbf{z}_m(n)$ that contain the transmitted

[1] As discussed later, as long as there is a bound on the order of the FIR channel, the physical layer guarantees symbol recovery (in the absence of noise). The channel order depends on the symbol rate, the carrier frequency, and the environment type, e.g., urban, hilly, indoor, etc. (see, e.g., [14], [22]).

symbols of user m corrupted by noise and the convolutive effects of the channels;

3) elimination of ISI using the filterbank $\mathbf{\Gamma}_m$.

We will show later on how recovery of $\mathbf{s}_m(i)$ can be guaranteed, regardless of the FIR channels. Before we proceed to a detailed description of our model, let us comment that our designs naturally address the downlink, where transmit antenna diversity is available at the base station. In the case of the uplink, if some mobile users have more than one transmit antennas, our designs can be applied there as well (but the users need to be quasisynchronized).

Detailed View: Our model represents signals, codes and channels by chip-rate samples of their complex envelopes. The information symbols $s_m(k)$ of user m are grouped together in blocks $\mathbf{s}_m(n) := \big(s_m(nK_m) \cdots s_m(nK_m + K_m - 1)\big)^{\mathrm{T}}$ of size K_m, which are mapped to blocks $\tilde{\mathbf{s}}_m(n) = \mathbf{\Theta}_m \mathbf{s}_m(n)$ of length J_m through the tall $J_m \times K_m$ matrix $\mathbf{\Theta}_m$ (the redundancy introduced by $\mathbf{\Theta}_m$ facilitates ISI elimination and symbol recovery, regardless of the physical channel [10], [26]). In practice, the precoder $\mathbf{\Theta}_m$ can be implemented either by a DSP processor and matrix operations or by a filterbank with K_m FIR filters $\theta_{m,k}(q)$, each of length J_m: $\theta_{m,k}(q) := [\mathbf{\Theta}_m]_{q,k}$. Then, the blocks $\tilde{\mathbf{s}}_m(n)$ are fed into the ST mapper $\mathcal{M}(\cdot)$, which takes two consecutive precoded blocks $\tilde{\mathbf{s}}_m(2n)$ and $\tilde{\mathbf{s}}_m(2n+1)$ to output the following $2J_m \times 2$ code matrix ($*$ denotes conjugation):

$$\begin{aligned}\mathbf{S}(n) &:= \begin{pmatrix} \bar{\mathbf{s}}_{m1}(2n) & \bar{\mathbf{s}}_{m1}(2n+1) \\ \bar{\mathbf{s}}_{m2}(2n) & \bar{\mathbf{s}}_{m2}(2n+1) \end{pmatrix} \\ &= \begin{pmatrix} \tilde{\mathbf{s}}_m(2n) & -\tilde{\mathbf{s}}_m^*(2n+1) \\ \tilde{\mathbf{s}}_m(2n+1) & \tilde{\mathbf{s}}_m^*(2n) \end{pmatrix} \begin{matrix} \rightarrow \\ \downarrow \end{matrix} \begin{matrix} \text{time} \\ \text{space.} \end{matrix} \end{aligned} \tag{1}$$

Each column corresponds to a transmission slot ("time"), whereas each row holds the symbols to be transmitted by each antenna ("space"). Note that without blocking (i.e., $J_m = 1$), the code matrix in (1) reduces to the ST block code in [2][2]. For notational convenience, we denote by $\bar{\mathbf{s}}_{mi}(n)$, $i = 1, 2$ the $J_m \times 1$ block transmitted through the ith transmit antenna at the time slot n and observe from (1) that, e.g., $\bar{\mathbf{s}}_{m1}(2n) = \tilde{\mathbf{s}}_m(2n)$, and $\bar{\mathbf{s}}_{m2}(2n+1) = \tilde{\mathbf{s}}_m^*(2n)$.

Instrumental in MUI elimination is the user-specific block-spreading code, which is represented by the $P \times J_m$ matrix $\mathbf{C}_m$. The user code is applied to $\bar{\mathbf{s}}_{mi}(n)$ to produce the block $\mathbf{u}_{mi}(n) := \mathbf{C}_m \bar{\mathbf{s}}_{mi}(n)$ of length P, which is transmitted by the mth user's ith antenna through the Lth-order FIR channel $\{h_{mi}(l)\}_{l=0}^{L}$. In order to eliminate the IBI caused by FIR channels, similar to OFDM, we rely on inserting a CP of length L at the beginning of $\mathbf{u}_{mi}(n)$; at the receiver, the corresponding first L received symbols are discarded. As explained in [26] and shown in Fig. 1, the CP insertion can be described by the transmit matrix $\mathbf{T}_{cp} := \big(\mathbf{I}_{cp}^{\mathrm{T}}\ \mathbf{I}_P^{\mathrm{T}}\big)^{\mathrm{T}}$, where $\mathbf{I}_{cp}$ is formed by the last L rows of the $P \times P$ identity matrix $\mathbf{I}_P$. Correspondingly, the receiver operation of discarding the first L received symbols is described by the receive-matrix $\mathbf{R}_{cp} := \big(\mathbf{0}_{P \times L}\ \mathbf{I}_P\big)$. The effect of the FIR channel $h_{mi}(l)$ on the transmitted data is described by the $(P+L) \times (P+L)$ Toeplitz (convolutional) matrix $\mathbf{H}_{mi}$ with first row $\big(h_{mi}(0)\mathbf{0}_{1 \times (P+L-1)}\big)$ and first column $\big(h_{mi}(0) \ldots h_{mi}(L)\mathbf{0}_{1 \times (P-1)}\big)^{\mathrm{T}}$. With $\tilde{\mathbf{H}}_{mi} := \mathbf{R}_{cp}\mathbf{H}_{mi}\mathbf{T}_{cp}$, the $P \times 1$ IBI-free received symbol block $\mathbf{y}(n)$ is given by (see Fig. 1)

$$\mathbf{y}(n) = \mathbf{x}_m(n) + \sum_{\mu=0,\, \mu \neq m}^{M-1} \mathbf{x}_\mu(n) + \mathbf{R}_{cp}\eta(n) \tag{2}$$

where $\mathbf{x}_m(n) := \tilde{\mathbf{H}}_{m1}\mathbf{C}_m\bar{\mathbf{s}}_{m1}(n) + \tilde{\mathbf{H}}_{m2}\mathbf{C}_m\bar{\mathbf{s}}_{m2}(n)$ denotes the received symbol block from the two transmit-antennas of the mth user, and $\eta(n)$ is the $(P+L) \times 1$ additive white Gaussian noise vector.

The received symbol block in (2) contains three terms.

1) The first term is the useful received block $\mathbf{x}_m(n)$ from the desired mth user.
2) The second term constitutes the MUI caused by simultaneous transmissions of the other $M-1$ users.
3) The third term is the additive noise.

Next, we present our code designs, which guarantee symbol recovery with diversity gains for each user, regardless of the MUI and underlying FIR channels. As a prelude to Section II-B, we note that the flexibility in assigning different information block length K_ms to different users enables our physical layer to support packet-level multirate services.

A. Code Design

To achieve improved BER performance at the physical layer, our system employs (pre)coding at three different levels:

1) *block-of-symbols* level (or lower level), where the tall precoder matrix $\mathbf{\Theta}_m$ combats ISI and guarantees symbol recovery, regardless of the FIR channels;
2) *transmit-antennae* level (or middle level), where the ST mapper is designed such that diversity gain at the receiver is guaranteed, regardless of the channel;
3) *user* level (or top level), where the code matrix $\mathbf{C}_m$ guarantees MUI elimination regardless of the FIR channels.

In the following, we describe our code design procedure starting from the top level and moving to the lower level.

Top Level—MUI Elimination: In order to design the code matrix $\mathbf{C}_m$ and the receive matrix $\mathbf{G}_m$, we will borrow some of the techniques of [26] to ensure that MUI is deterministically eliminated while still guaranteeing symbol recovery for user m. The designs in [26] are for single-transmit antenna and capitalize on block-spreading and the core concept of subcarrier allocation. Similar to OFDMA, every user m is allocated a distinct set of J_m subcarriers to transmit information, but unlike OFDMA, the all-digital framework of [26] guarantees symbol recovery, irrespective of channel nulls. One of the fundamental insights of [26] is that an Lth-order FIR channel manifests itself as at most L deep fades on the FFT grid. Hence, when the channel is not known to the transmitter, even in the noiseless case, source symbols transmitted on L (out of the possible J_m) subcarriers may be lost; this potential loss is taken care of by our inner code. Herein, we allocate J_m subcarriers to every user m; these subcarriers are used by both transmit antennas to produce two interfering signals at the receiver end (something that [26] did not have to cope with). For the time being, we focus on eliminating

[2]However, the similarities end there; the technique in [2] was designed for flat fading channels, whereas our space-time mapper targets spectrally shaped channels and take into account the linear precoder $\mathbf{\Theta}_m$.

MUI, leaving it up to our ST coding to take care of the two interfering signals generated by user m. Note also that both antennas transmit at the same time.

With a P-long FFT grid, there are P subcarriers, which are represented in the discrete-time equivalent baseband model as $\exp(j2\pi p/P)$, $p = 0, 1, \ldots, P-1$. Each user is allocated J_m distinct subcarriers, with $\sum_{m=0}^{M-1} J_m = P$. The subcarriers are represented as indices in the set $\mathcal{J}_m$, and the user is allowed to transmit information only the subcarriers $\{\exp(j2\pi p/P)\}_{p\in\mathcal{J}_m}$.[3] As a result, the matrices $\mathbf{C}_m$, $\mathbf{G}_m$ are defined in terms of the $P \times P$ FFT matrix $\mathbf{F}$ and the $P \times J_m$ subcarrier selector matrix $\mathbf{\Phi}_m$ as follows: $\mathbf{C}_m = \mathbf{F}^{\mathcal{H}}\mathbf{\Phi}_m$, $\mathbf{G}_m = \mathbf{\Phi}_m^{\mathrm{T}}\mathbf{F}$, $m = 0, \ldots, M-1$. The (k,p) entry of the $P \times P$ FFT matrix $\mathbf{F}$ is defined as $[\mathbf{F}]_{k,p} = P^{-(1/2)}\exp\{(-j2\pi kp)/P\}$, whereas the $P \times J_m$ subcarrier selector matrix $\mathbf{\Phi}_m$ is comprised of the $\mathcal{J}_m$ columns of the $P \times P$ identity matrix $\mathbf{I}_P$. The matrix $\mathbf{\Phi}_m$ forces user m to transmit information only on subcarriers allocated to user m; at the receiver end, only these subcarriers are taken into account for the recovery of the transmitted symbols. Then, it can be seen [26] that the receive-filter output $\mathbf{y}_m(n)$ can be written as

$$\mathbf{y}_m(n) = \sum_{\mu=0}^{M-1} \mathbf{\Phi}_m^{\mathrm{T}}\mathbf{F}\Big[\tilde{\mathbf{H}}_{\mu 1}\mathbf{F}^{\mathcal{H}}\mathbf{\Phi}_\mu \bar{\mathbf{s}}_{\mu 1}(n) + \tilde{\mathbf{H}}_{\mu 2}\mathbf{F}^{\mathcal{H}}\mathbf{\Phi}_\mu \bar{\mathbf{s}}_{\mu 2}(n)\Big] + \mathbf{G}_m\mathbf{R}_{cp}\eta(n) \quad (3)$$

which yields

$$\mathbf{y}_m(n) = \mathcal{D}_{m1}\bar{\mathbf{s}}_{m1}(n) + \mathcal{D}_{m2}\bar{\mathbf{s}}_{m2}(n) + \mathbf{G}_m\mathbf{R}_{cp}\boldsymbol{\eta}(n) \quad (4)$$

where $\mathcal{D}_{mi}$ is a $J_m \times J_m$ diagonal matrix holding the frequency response of the channel $h_{mi}(l)$ at the J_m subcarriers of user m: $\mathcal{D}_{mi} = \mathrm{diag}[H_{mi}(\rho_{m,0}), \ldots, H_{mi}(\rho_{m,j_m})]$, $H_{mi}(\rho) := \sum_{l=0}^{L} h(l)\rho^{-l}$. It is clear from (4) that the MUI has been eliminated through the joint design of $\mathbf{C}_\mu$ and $\mathbf{G}_\mu$. Note also that MUI elimination is achieved without requiring the knowledge of the channel impulse response (CIR) at the receiver. Furthermore, with an interleaved subcarrier assignment [26], the corresponding fading coefficients at every subcarrier are less likely to be correlated; although the interleaved subcarrier assignment does not change the diversity order,[4] it can improve the BER performance of the system. However, it is well known that multicarrier transmissions are sensitive to frequency offsets (and Doppler), and a lot of work has been done (by many researchers) to mitigate this problem; addressing this problem is beyond the scope of this paper (in our simulations, we will assume perfect frequency synchronization).

Having eliminated the MUI, we exploit next the ST coding in (1) to recover the transmitted symbols $\mathbf{s}_m(n)$ with guaranteed diversity gains.

Diversity Gain: The objective of the middle-level code is to collect diversity gains by combining constructively the transmitted signals from the two antennas. Knowing $\mathcal{D}_{m1}$ and $\mathcal{D}_{m2}$, we consider two consecutive MUI-free blocks: $\mathbf{y}_m(2n)$ and $\mathbf{y}_m(2n+1)$. Recall that $\tilde{\mathbf{s}}_m(n)$ is mapped to $\bar{\mathbf{s}}_{mi}(n)$ as

$$\begin{aligned} \bar{\mathbf{s}}_{m1}(2n) &\longleftrightarrow \tilde{\mathbf{s}}_m(2n) \\ \bar{\mathbf{s}}_{m2}(2n) &\longleftrightarrow \tilde{\mathbf{s}}_m(2n+1) \\ \bar{\mathbf{s}}_{m1}(2n+1) &\longleftrightarrow -\tilde{\mathbf{s}}_m^*(2n+1) \\ \bar{\mathbf{s}}_{m2}(2n+1) &\longleftrightarrow \tilde{\mathbf{s}}_m^*(2n). \end{aligned} \quad (5)$$

Plugging the mapping (5) into (4), we express $\mathbf{y}_m(2n)$ and $\mathbf{y}_m(2n+1)$ as

$$\begin{aligned} \mathbf{y}_m(2n) =& \mathcal{D}_{m1}\tilde{\mathbf{s}}_m(2n) + \mathcal{D}_{m2}\tilde{\mathbf{s}}_m(2n+1) \\ &+ \mathbf{G}_m\mathbf{R}_{cp}\boldsymbol{\eta}(2n) \quad (6a) \\ \mathbf{y}_m(2n+1) =& -\mathcal{D}_{m1}\tilde{\mathbf{s}}_m^*(2n+1) + \mathcal{D}_{m2}\tilde{\mathbf{s}}_m^*(2n) \\ &+ \mathbf{G}_m\mathbf{R}_{cp}\boldsymbol{\eta}(2n+1). \quad (6b) \end{aligned}$$

In order to exploit the embedded diversity of (6a) and (6b), we design the ST decoder $\bar{\mathcal{M}}(\cdot)$ (see Fig. 1) by forming its two consecutive output blocks $\mathbf{z}_m(2n)$ and $\mathbf{z}_m(2n+1)$ as

$$\begin{pmatrix} \mathbf{z}_m(2n) \\ \mathbf{z}_m(2n+1) \end{pmatrix} = \begin{pmatrix} \mathcal{D}_{m1}^* & \mathcal{D}_{m2} \\ \mathcal{D}_{m2}^* & -\mathcal{D}_{m1} \end{pmatrix} \begin{pmatrix} \mathbf{y}_m(2n) \\ \mathbf{y}_m^*(2n+1) \end{pmatrix}. \quad (7)$$

Substituting (6a) and (6b) into (7), we arrive at

$$\mathbf{z}_m(n) = [\mathcal{D}_{m1}^*\mathcal{D}_{m1} + \mathcal{D}_{m2}^*\mathcal{D}_{m2}]\,\tilde{\mathbf{s}}_m(n) + \tilde{\boldsymbol{\eta}}_m(n) \quad (8)$$

where the additive noise vector $\tilde{\boldsymbol{\eta}}_m(n) := [\boldsymbol{\eta}_m^{\mathrm{T}}(2n)\boldsymbol{\eta}_m^{\mathrm{T}}(2n+1)]^{\mathrm{T}}$ is given by

$$\tilde{\boldsymbol{\eta}}_m(n) := \begin{pmatrix} \mathcal{D}_{m1}^* & \mathcal{D}_{m2} \\ \mathcal{D}_{m2}^* & -\mathcal{D}_{m1} \end{pmatrix} \begin{pmatrix} \mathbf{G}_m\mathbf{R}_{cp}\boldsymbol{\eta}(2n) \\ \mathbf{G}_m^*\mathbf{R}_{cp}\boldsymbol{\eta}^*(2n+1) \end{pmatrix}. \quad (9)$$

If the receiver noise is temporally white, then $\boldsymbol{\eta}(n)$ is a white Gaussian random process with covariance matrix $\sigma_\eta^2\,\mathbf{I}_{P+L}$. It readily follows that the covariance matrix of $\tilde{\boldsymbol{\eta}}_m(n)$ is given by

$$\mathrm{Cov}(\tilde{\boldsymbol{\eta}}_m) = \sigma_\eta^2 \cdot \begin{pmatrix} \mathcal{D}_{m1}^*\mathcal{D}_{m1} + \mathcal{D}_{m2}^*\mathcal{D}_{m2} & \mathbf{0}_{J_m\times J_m} \\ \mathbf{0}_{J_m\times J_m} & \mathcal{D}_{m1}^*\mathcal{D}_{m1} + \mathcal{D}_{m2}^*\mathcal{D}_{m2} \end{pmatrix}. \quad (10)$$

Because $\mathcal{D}_{mi}$, $i = 1, 2$ are diagonal matrices, we infer from (10) that the entries of $\tilde{\boldsymbol{\eta}}_m(n)$ are independent. As a result, the blocks $\mathbf{z}_m(n)$ can be processed individually without loss in performance. To show how the transmit-diversity gains are achieved, we plug (4) into (8), to obtain

$$\begin{aligned} \mathbf{z}_m(n) =& \mathcal{D}_m\tilde{\mathbf{s}}_m(n) + \boldsymbol{\eta}_m(n) \\ =& \mathcal{D}_m\mathbf{\Theta}_m\mathbf{s}_m(n) + \boldsymbol{\eta}_m(n) \end{aligned} \quad (11)$$

where $\mathcal{D}_m := \mathcal{D}_{m1}^*\mathcal{D}_{m1} + \mathcal{D}_{m2}^*\mathcal{D}_{m2} = \mathrm{diag}[\sum_{i=1}^{2}|H_{mi}(\rho_{m,1})|^2, \ldots, \sum_{i=1}^{2}|H_{mi}(\rho_{m,J_m})|^2]$.

As each channel can have at most L nulls, (11) implies that transmit-diversity gains are achieved in at least $J_m - 2L$ subcarriers. Moreover, $J_m - L$ subcarriers are guaranteed to be nonzero and can be used for symbol recovery (regardless of the underlying channels). The latter observation brings us to the lower-level component of our (pre)coding.

Guaranteed Symbol Recovery We deduce from (11) that the recovery of $\mathbf{s}_m(n)$ from $\mathbf{z}_m(n)$ requires $\mathcal{D}_m\mathbf{\Theta}_m$ to be full column rank. As shown in [6], [10], [25], [26], the full

[3]For example, if user m is allocated the indices $\{10, \ldots, 20\}$, then user m is allowed to transmit information only on subcarriers $\exp(j2\pi 10/P), \ldots, \exp(j2\pi 20/P)$.

[4]We thank the anonymous reviewers for pointing this out to us.

column rank is guaranteed by selecting i) $J_m = K_m + L$ and ii) any K_m rows of $\boldsymbol{\Theta}_m$ to be linearly independent. To satisfy conditions i) and ii), a special choice of $\boldsymbol{\Theta}_m$ is given by [6], [26]

$$\boldsymbol{\Theta}_m = \begin{pmatrix} 1 & \rho_{m,0}^{-1} & \cdots & \rho_{m,0}^{-(K_m-1)} \\ \vdots & & & \vdots \\ 1 & \rho_{m,J_m-1}^{-1} & \cdots & \rho_{m,J_m-1}^{-(K_m-1)} \end{pmatrix}. \quad (12)$$

Linear precoding (which can be viewed as coding over the complex field) as opposed to channel coding (done over the $GF(q)$) does not appear, at first glance, to offer any significant advantages. The work in [8] and [27] highlight the merits of precoding (for communications over frequency selective channels) and includes illustrative simulations that demonstrate the improved BER performance that can be achieved with precoding. We also note that in a practical system, linear precoding does *not* replace channel coding; rather, it can be used to enhance the BER performance, which is achieved with traditional channel coding schemes (such as convolutional codes).

At the transmitter, our code assignment procedure can be thought of as a mapping of M signal spaces (each of dimension K_m) to M orthogonal subspaces of a P-dimensional signal space. The orthogonality of these subspaces is not affected by the $2M$ convolutive channels, and at the receiver, MUI is eliminated by projecting the signal back to M subspaces, each of dimension J_m. Effectively, the mth user's K_m-dimensional subspace is mapped to a J_m-dimensional subspace. If the channels (corresponding to the m-th user) do not have any zeros on the unit circle, then all J_m dimensions can be used for the recovery of the K_m transmitted symbols (frequency diversity). Whenever a channel has a null on a specific subcarrier, then the corresponding dimension (in the J_m-dimensional signal space) is "lost"; the remaining "intact" dimensions are used for the recovery of the transmitted symbols. To increase the reliability of the symbol estimates, our ST decoder adds coherently the signal components of the two J_m-dimensional subspaces (which correspond to the two transmit antennas). From the viewpoint of diversity gains, the worst case occurs when $2L$ dimensions are lost. From the viewpoint of symbol recovery, the worst case occurs when the two channels have zeros at the same L subcarriers, which leaves only $J_m - L$ dimensions for symbol recovery. Thus, by setting $K_m = J_m - L$, we guarantee that there are enough dimensions for symbol recovery, even in the worst case. Furthermore, in at least $J_m - 2L$ dimensions, our ST code achieves diversity gains. Lacking the linear precoder $\boldsymbol{\Theta}_m$, we note that [1] cannot guarantee symbol recovery. As we will illustrate by simulations (Section IV), these diversity gains result in significant BER improvements and SNR savings.

B. Supporting Integrated Services

The fact that the mth user's transmission rate is $K_m/(P+L)$ reveals another attractive feature of our designs, namely, multirate allocation with arbitrarily fine resolution (as we increase P). In an integrated services framework, the flexibility in assigning values to J_m allows the physical layer to implement bandwidth allocation as specified by the network layer scheduler.[5] To appreciate the importance of a multirate-transparent physical layer, we should take into consideration that nowadays, a large class of QoS network schedulers are based on the generalized processor sharing (GPS) [13] scheduling policy. According to GPS, every user m should be allocated bandwidth proportional to a user-specific positive weight ϕ_m. As shown in [17], multirate transmissions at the physical layer enable fair bandwidth allocation at the network layer without resorting to TDMA. The basic idea is that in every transmission round, each user m is allocated a portion BW_m of the total bandwidth BW according to $\text{BW}_m/\text{BW} = \phi_m / \sum_{\mu \in \mathcal{A}} \phi_\mu$, where $\mathcal{A}$ is the set of active users. By setting

$$J_m = \left\lfloor \frac{\text{BW}_m}{\text{BW}} P \right\rfloor, \quad K_m = J_m - L$$

we ensure that the bandwidth assignments as dictated by the network layer are implemented at the physical layer. Hence, our code assignment procedure could also play a very important role in translating BER improvements at the physical layer to throughput improvements at the network layer. This is because in each transmission round, every mobile user is assigned its fair share of the bandwidth and can immediately exploit any BER gains at the physical layer.

Before we present how our framework can utilize multiple receive antennas, we would like to reiterate that if one wants to dispense with TDMA and still provide integrated services, then the physical layer should possess multirate/multiuser capabilities. The subcarrier-allocation scheme of [6], [10], [25], and [26] is not the only physical layer framework capable of providing such services. Multicode schemes (based on orthogonal variable-spreading codes or multiple pseudonoise codes) can also support different transmission rates and multiple users [9], [20]. However, pseudonoise codes do not guarantee deterministic MUI elimination, and orthogonal codes (at the transmitter) may not be orthogonal at the receiver (because of the effect of the convolutive FIR channels [26]). Thus, in broadband wireless networks, where unknown frequency-selective multipath naturally arises, the multicarrier framework of [6], [10], [25], and [26] is well-motivated for improved BER performance.

III. Space-Time CDMA With Two Receive Antennas

In a single-user environment, it is well known that more reliable symbol estimates can be obtained using more than one receive antenna. If we recall that in our system that subcarrier allocation converts the multiuser environment to a single-user one, then single-user array-processing algorithms could be applied to our framework (with a few modifications) to improve the BER if the receiver is equipped with $N_r > 1$ antennas. As we demonstrate in the simulations section, this is indeed the case in our framework. However, in a multiuser environment, multiple receive antennas can also be used for user separation; for example, M users can be separated at the receiver using M receive antennas. Hence, the presence of multiple receive antennas could be taken into account in the design of the outer code.

[5]The network layer scheduler has a profound effect on the quality of service (QoS) guarantees that can be provided to users since it is the scheduler the one who determines the transmission order of packets in the network.

The key idea we pursue in this section is that two users μ and m with same transmission rates ($J_m = J_\mu = J$) may share the same set of subcarriers and be separated using array processing. Before we study how user separation with multiple receive antennas can be accomplished, let us comment on the features of such a scheme. On the one hand, subcarrier sharing effectively doubles the transmission rate of users m and μ. With a single receive antenna, each user is allocated J subcarriers, whereas with two receive antennas, each user is allocated $2J$ subcarriers; hence, in every transmission round, the two users could transmit (almost) twice as many symbols. On the other hand, subcarrier sharing could impose a BER (and thus an SNR) penalty because user separation based on array processing may not be as successful as the deterministic MUI elimination (which is based on allocation of disjoint subcarrier sets). Indeed, in the extreme case, the symbol recovery is no longer guaranteed when multiple receive antennas are employed to separate users. However, in the simulations section, we will see that the BER penalty by subcarrier sharing is quite small; this is because the aforementioned extreme case occurs at probability zero.

In more detail, when users m and μ have been allocated the same subcarriers, then after eliminating the other users, the received signal in the first antenna is (cf. (4))

$$\begin{aligned}\mathbf{y}_{m,\mu}(n) =& \underbrace{\boldsymbol{\mathcal{D}}_{m1}\bar{\mathbf{s}}_{m1}(n) + \boldsymbol{\mathcal{D}}_{m2}\bar{\mathbf{s}}_{m2}(n)}_{\text{user } m} \\ &+ \underbrace{\boldsymbol{\mathcal{D}}_{\mu 1}\bar{\mathbf{s}}_{\mu 1}(n) + \boldsymbol{\mathcal{D}}_{\mu 2}\bar{\mathbf{s}}_{\mu 2}(n)}_{\text{user } \mu} \\ &+ \mathbf{G}_{m,\mu}\mathbf{R}_{cp}\boldsymbol{\eta}(n). \end{aligned} \tag{13}$$

Although our designs can be generalized for $N_r > 2$ antennas, let us focus in the case of two receive antennas. Using the prime ($'$) to denote channels and received signals corresponding to the second receive antenna, we obtain

$$\begin{aligned}\mathbf{y}'_{m,\mu}(n) =& \underbrace{\boldsymbol{\mathcal{D}}'_{m1}\bar{\mathbf{s}}_{m1}(n) + \boldsymbol{\mathcal{D}}'_{m2}\bar{\mathbf{s}}_{m2}(n)}_{\text{user } m} \\ &+ \underbrace{\boldsymbol{\mathcal{D}}'_{\mu 1}\bar{\mathbf{s}}_{\mu 1}(n) + \boldsymbol{\mathcal{D}}'_{\mu 2}\bar{\mathbf{s}}_{\mu 2}(n)}_{\text{user } \mu} \\ &+ \mathbf{G}_{m,\mu}\mathbf{R}_{cp}\boldsymbol{\eta}'(n). \end{aligned} \tag{14}$$

By taking into account the ST mapping of (1) and (5), we obtain

$$\underbrace{\begin{pmatrix} \mathbf{y}_{m,\mu}(2n) \\ \mathbf{y}^*_{m,\mu}(2n+1) \\ \mathbf{y}'_{m,\mu}(2n) \\ \mathbf{y}'^*_{m,\mu}(2n+1) \end{pmatrix}}_{\mathbf{y}} = \underbrace{\begin{pmatrix} \begin{pmatrix} \boldsymbol{\mathcal{D}}_{m1} & \boldsymbol{\mathcal{D}}_{m2} \\ \boldsymbol{\mathcal{D}}^*_{m2} & -\boldsymbol{\mathcal{D}}^*_{m1} \end{pmatrix} & \begin{pmatrix} \boldsymbol{\mathcal{D}}_{\mu 1} & \boldsymbol{\mathcal{D}}_{\mu 2} \\ \boldsymbol{\mathcal{D}}^*_{\mu 2} & -\boldsymbol{\mathcal{D}}^*_{\mu 1} \end{pmatrix} \\ \begin{pmatrix} \boldsymbol{\mathcal{D}}'_{m1} & \boldsymbol{\mathcal{D}}'_{m2} \\ \boldsymbol{\mathcal{D}}'^*_{m2} & -\boldsymbol{\mathcal{D}}'^*_{m1} \end{pmatrix} & \begin{pmatrix} \boldsymbol{\mathcal{D}}'_{\mu 1} & \boldsymbol{\mathcal{D}}'_{\mu 2} \\ \boldsymbol{\mathcal{D}}'^*_{\mu 2} & -\boldsymbol{\mathcal{D}}'^*_{\mu 1} \end{pmatrix} \end{pmatrix}}_{\mathbf{H}}$$

$$\times \underbrace{\begin{pmatrix} \tilde{\mathbf{s}}_m(2n) \\ \tilde{\mathbf{s}}_m(2n+1) \\ \tilde{\mathbf{s}}_\mu(2n) \\ \tilde{\mathbf{s}}_\mu(2n+1) \end{pmatrix}}_{\tilde{\mathbf{s}}} + \underbrace{\begin{pmatrix} \mathbf{G}_{m,\mu}\mathbf{R}_{cp}\boldsymbol{\eta}(2n) \\ \mathbf{G}_{m,\mu}\mathbf{R}_{cp}\boldsymbol{\eta}(2n+1) \\ \mathbf{G}_{m,\mu}\mathbf{R}_{cp}\boldsymbol{\eta}'(2n) \\ \mathbf{G}_{m,\mu}\mathbf{R}_{cp}\boldsymbol{\eta}'(2n+1) \end{pmatrix}}_{\mathbf{n}} \tag{15}$$

which, for compactness, we write as

$$\boldsymbol{y} = \boldsymbol{H}\tilde{\boldsymbol{s}} + \boldsymbol{n} \tag{16}$$

where the vectors $\boldsymbol{y}$, $\tilde{\boldsymbol{s}}$, and $\boldsymbol{n}$ are $4J \times 1$, and the matrix $\boldsymbol{H}$ is $4J \times 4J$. Note also that the diagonal "$\boldsymbol{\mathcal{D}}$" matrices in (13) and (14) make each of the $2J \times 2J$ submatrices $\boldsymbol{H}_{1,1}$, $\boldsymbol{H}_{1,2}$, $\boldsymbol{H}_{2,1}$, $\boldsymbol{H}_{2,2}$ of

$$\boldsymbol{H} = \begin{pmatrix} \boldsymbol{H}_{1,1} & \boldsymbol{H}_{1,2} \\ \boldsymbol{H}_{2,1} & \boldsymbol{H}_{2,2} \end{pmatrix}$$

have the special structure shown in (15). It is naturally expected that users m, μ will also share the same linear precoder, which is denoted by $\boldsymbol{\Theta}_{m,\mu}$. Therefore, (16) can also be written as

$$\boldsymbol{y} = \tilde{\boldsymbol{H}}\boldsymbol{s} + \boldsymbol{n} \tag{17}$$

where $\tilde{\boldsymbol{H}} := \boldsymbol{H}\ (\mathbf{I}_{4J} \otimes \boldsymbol{\Theta}_{m,\mu})$, and $\boldsymbol{s} := \left(\mathbf{s}^{\mathrm{T}}_m(2n)\mathbf{s}^{\mathrm{T}}_m(2n+1)\mathbf{s}^{\mathrm{T}}_\mu(2n)\mathbf{s}^{\mathrm{T}}_\mu(2n+1)\right)^{\mathrm{T}}$. Let us see now how the transmitted symbols can be recovered from (16) [or (17)].

A. Linear and DF Receivers

If the receive antennas are well separated, the underlying physical channels are independent, and the matrices $\boldsymbol{H}$, $\tilde{\boldsymbol{H}}$ are full column rank. Then, a number of techniques can be applied to (16) to recover the transmitted symbols. For example, [15] offers closed-form ZF and MMSE receiver designs, whereas [18] suggests a block decision feedback (DF) approach for improved BER. According to [15], the ZF receiver can be implemented by the filterbank $\boldsymbol{\Gamma}_{zf} = \boldsymbol{H}^\dagger$ (the pseudoinverse of $\boldsymbol{H}$), whereas the MMSE receiver is given by $\boldsymbol{\Gamma}_{mmse} = \mathbf{R}_{\tilde{s}\tilde{s}}\boldsymbol{H}^{\mathcal{H}}(\mathbf{R}_{nn} + \boldsymbol{H}\mathbf{R}_{\tilde{s}\tilde{s}}\boldsymbol{H}^{\mathcal{H}})^{-1}$, where $\mathbf{R}_{\tilde{s}\tilde{s}} := E\{\tilde{\boldsymbol{s}}\tilde{\boldsymbol{s}}^{\mathcal{H}}\}$, $\mathbf{R}_{nn} := E\{\boldsymbol{n}\boldsymbol{n}^{\mathcal{H}}\}$ is the autocorrelation of $\tilde{\boldsymbol{s}}$ and $\boldsymbol{n}$, respectively. On the other hand, the DF designs of [18] are based on two filterbanks described by the matrices $\mathbf{W}$, $\mathbf{B}$, which implement the feedforward and the feedback part of the DF receiver (as depicted in Fig. 2). The ZF-DF receiver $(\mathbf{W}_{zf}, \mathbf{B}_{zf})$ is given by $\mathbf{W}_{zf} = \mathbf{D}^{-1}_{zf}\mathbf{U}^{-\mathcal{H}}_{zf}\tilde{\boldsymbol{H}}^{\mathcal{H}}\mathbf{R}^{-1}_{nn}$, $\mathbf{B}_{zf} = \mathbf{U} - \mathbf{I}_{4J}$, where $\mathbf{U}_{zf}$ is an upper triangular matrix with unit diagonal given by the Cholesky factorization of the matrix $\tilde{\boldsymbol{H}}^{\mathcal{H}}\mathbf{R}^{-1}_{nn}\tilde{\boldsymbol{H}} = \mathbf{U}^{\mathcal{H}}_{zf}\mathbf{D}_{zf}\mathbf{U}_{zf}$ and $\mathbf{D}_{zf}$ a diagonal matrix. The MMSE-DF $(\mathbf{W}_{mmse}, \mathbf{B}_{mmse})$ receiver takes into account both $\mathbf{R}_{sy} := E\{\boldsymbol{s}\boldsymbol{y}^{\mathcal{H}}\}$ and $\mathbf{R}_{yy} = \mathbf{R}_{nn} + \tilde{\boldsymbol{H}}\mathbf{R}_{ss}\tilde{\boldsymbol{H}}^{\mathcal{H}}$,

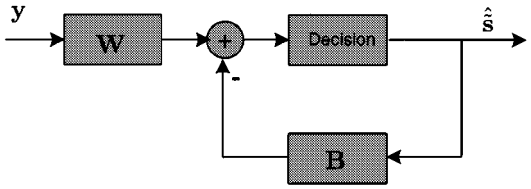

Fig. 2. DF receiver.

and its settings are given by $\mathbf{W}_{mmse} = \mathbf{U}_{mmse}\mathbf{R}_{sy}\mathbf{R}_{yy}^{-1}$, $\mathbf{B}_{mmse} = \mathbf{U}_{mmse} - \mathbf{I}_{4J}$, where $\mathbf{U}_{mmse}$ is an upper triangular matrix with unit diagonal given by the Cholesky factorization of $\mathbf{R}_{ss}^{-1} + \tilde{\boldsymbol{H}}^{\mathcal{H}}\mathbf{R}_{nn}^{-1}\tilde{\boldsymbol{H}} = \mathbf{U}_{mmse}^{\mathcal{H}}\mathbf{D}_{mmse}\mathbf{U}_{mmse}$ and $\mathbf{D}_{mmse}$ a diagonal matrix. The DF receivers exploit the finite alphabet of the transmitted symbols and the whiteness of the noise at the input of the decision device (noise whitening is made possible by the proper setting of the feedforward filter). As a result, for $N_r = N_t = 1$ (no ST coding), the DF receivers outperform their linear counterparts both in the single-user case [18] and in the multiuser case [8]. However, both the linear and the DF receivers do not exploit the special structure of $\boldsymbol{H}$ in (15).

B. Linear Two-Stage ST Receiver

We next propose a linear two-stage ST receiver that takes advantage of the ST code structure. To see how this receiver works, let us define the linear filter $\boldsymbol{W}$ as

$$\boldsymbol{W} := \begin{pmatrix} \mathbf{I}_{2J} & -\boldsymbol{H}_{1,2}\boldsymbol{H}_{2,2}^{-1} \\ -\boldsymbol{H}_{2,1}\boldsymbol{H}_{1,1}^{-1} & \mathbf{I}_{2J} \end{pmatrix}. \tag{18}$$

Our receiver decodes the information symbols in two steps. First, the linear filter $\boldsymbol{W}$ is applied to $\boldsymbol{y}$ to produce the MUI-free $(\boldsymbol{y}_m^{\mathrm{T}}\ \boldsymbol{y}_\mu^{\mathrm{T}})^{\mathrm{T}}$ as in (19), shown at the bottom of the page, where $(\boldsymbol{n}_1^{\mathrm{T}}\ \boldsymbol{n}_2^{\mathrm{T}})^{\mathrm{T}} := \boldsymbol{W}\boldsymbol{n}$. Second, the symbols of users m and μ are recovered from the $2J \times 1$ vectors $\boldsymbol{y}_m$ and $\boldsymbol{y}_\mu$:

$$\boldsymbol{y}_m = \left(\boldsymbol{H}_{1,1} - \boldsymbol{H}_{1,2}\boldsymbol{H}_{2,2}^{-1}\boldsymbol{H}_{2,1}\right)\begin{pmatrix} \tilde{\mathbf{s}}_m(2n) \\ \tilde{\mathbf{s}}_m(2n+1) \end{pmatrix} + \boldsymbol{n}_1 \tag{20a}$$

$$\boldsymbol{y}_\mu = \left(\boldsymbol{H}_{2,2} - \boldsymbol{H}_{2,1}\boldsymbol{H}_{1,1}^{-1}\boldsymbol{H}_{1,2}\right)\begin{pmatrix} \tilde{\mathbf{s}}_\mu(2n) \\ \tilde{\mathbf{s}}_\mu(2n+1) \end{pmatrix} + \boldsymbol{n}_2. \tag{20b}$$

As proved in the Appendix, the matrices $\boldsymbol{H}_{1,1} - \boldsymbol{H}_{1,2}\boldsymbol{H}_{2,2}^{-1}\boldsymbol{H}_{2,1}$ and $\boldsymbol{H}_{2,2} - \boldsymbol{H}_{2,1}\boldsymbol{H}_{1,1}^{-1}\boldsymbol{H}_{1,2}$ can be written as

$$\begin{aligned} \boldsymbol{H}_{1,1} - \boldsymbol{H}_{1,2}\boldsymbol{H}_{2,2}^{-1}\boldsymbol{H}_{2,1} &= \begin{pmatrix} \mathbf{A}_m & \mathbf{B}_m \\ \mathbf{B}_m^* & -\mathbf{A}_m^* \end{pmatrix} \\ \boldsymbol{H}_{2,2} - \boldsymbol{H}_{2,1}\boldsymbol{H}_{1,1}^{-1}\boldsymbol{H}_{1,2} &= \begin{pmatrix} \mathbf{A}_\mu & \mathbf{B}_\mu \\ \mathbf{B}_\mu^* & -\mathbf{A}_\mu^* \end{pmatrix} \end{aligned} \tag{21}$$

where $\mathbf{A}_m, \mathbf{B}_m, \mathbf{A}_\mu, \mathbf{B}_\mu\mathbf{A}_m$, $\mathbf{B}_m$, $\mathbf{A}_\mu$, and $\mathbf{B}_\mu$ are $J \times J$ diagonal matrices. Given (21), we can see that, e.g., $\boldsymbol{y}_m$ of (20a) can be broken into two parts [similar to (6a) and (6b)]:

$$\boldsymbol{y}_m = \begin{pmatrix} \mathbf{A}_m & \mathbf{B}_m \\ \mathbf{B}_m^* & -\mathbf{A}_m^* \end{pmatrix}\begin{pmatrix} \tilde{\mathbf{s}}_m(2n) \\ \tilde{\mathbf{s}}_m(2n+1) \end{pmatrix} + \boldsymbol{n}_1. \tag{22}$$

Hence, the symbols of user m can be retrieved with ST diversity gains following the path dictated by (7) and (8). Different from (6a) and (6b), where at most L diagonal entries of $\mathcal{D}_{m1}$ and $\mathcal{D}_{m2}$ could be zeros, the diagonal matrices $\mathbf{A}_m$ and $\mathbf{B}_m$ could be zero matrices due to the array processing. Thus, symbol recovery is no longer guaranteed when array processing is performed to separate users m and μ.

From a maximum likelihood estimation standpoint, disjoint symbol recovery for users m and μ is not optimal. It can be seen that $\boldsymbol{W}\boldsymbol{W}^{\mathcal{H}}$ is not diagonal, which makes $\boldsymbol{n}$ colored (i.e., $\boldsymbol{n}_1, \boldsymbol{n}_2$ are dependent). Therefore, subcarrier sharing comes with a price to be paid both in the form of suboptimum symbol estimation and in the form of possibly reduced SNR as evinced by the factors $-\boldsymbol{H}_{1,2}\boldsymbol{H}_{2,2}^{-1}\boldsymbol{H}_{2,1}$ and $-\boldsymbol{H}_{2,1}\boldsymbol{H}_{1,1}^{-1}\boldsymbol{H}_{1,2}$ in (20a) and (20b), respectively. We note that the form of $\boldsymbol{W}$ is reminiscent of the matrix linear combiner of [12, (24)] but with a few important differences. First, the pertinent method in [12] assumes flat-fading channels, whereas we take into account the channel order. Second, our block matrices $\boldsymbol{H}_{1,1}$, $\boldsymbol{H}_{1,2}$, $\boldsymbol{H}_{2,1}$, and $\boldsymbol{H}_{2,2}$ hold the frequency response of the channels (at the corresponding subcarriers), whereas in [12], the block submatrices hold the fading constants of the flat fading channels.

The results of this section are in agreement with the theory of [21] (developed for flat-fading channels). As it is illustrated in the Simulations section, the bit-error-performance of the system with two-receive-antennas and two users sharing the same subcarriers is approximately the same as that of the system with one receive antenna. Hence, diversity loss *did* occur in the system with the two-receive-antennas as, intuitively thinking, the extra degree of freedom provided by the second antenna is used for the separation of the two users. However, the two-stage ST receiver does not decrease the transmit diversity [as indicated by (22)], which is a fact that is also verified by our simulation results.

Having designed our receiver, we next resort to simulations to investigate the performance of our designs.

IV. Simulations

In this section, we present simulation results for $N_r = 1$ and $N_r = 2$ receive antennas. When all mobile users have been assigned the same rates, [10] provides simulations that show the benefits of ST coding. Herein, we are interested in the multirate aspects of our framework and the way in which our designs improve on the single-transmit/single-receive antenna scenario (which amounts to no spatial diversity). Our results provide testament to the (intuitive) fact that, starting from a single transmit- and receive-antenna, the addition of a second transmit-antenna improves the BER performance significantly, and further improvement can be achieved by deploying a second receive-antenna. We will corroborate here that as we add more antenna hardware, we do not lose any of the multiuser/multirate strengths of [26].

We study a system with $M = 8$ users, where each user is equipped with two transmit-antennas; two high-rate users have been assigned the weight $\phi_{hr} \approx 1/4$, and two middle-rate users have $\phi_{mr} \approx 1/8$, whereas four low-rate users have been

$$\begin{pmatrix} \boldsymbol{y}_m \\ \boldsymbol{y}_\mu \end{pmatrix} := \boldsymbol{W}\boldsymbol{y} \overset{(16)}{=} \begin{pmatrix} \boldsymbol{H}_{1,1} - \boldsymbol{H}_{1,2}\boldsymbol{H}_{2,2}^{-1}\boldsymbol{H}_{2,1} & \mathbf{0}_{2J} \\ \mathbf{0}_{2J} & \boldsymbol{H}_{2,2} - \boldsymbol{H}_{2,1}\boldsymbol{H}_{1,1}^{-1}\boldsymbol{H}_{1,2} \end{pmatrix}\tilde{\boldsymbol{s}} + \begin{pmatrix} \boldsymbol{n}_1 \\ \boldsymbol{n}_2 \end{pmatrix} \tag{19}$$

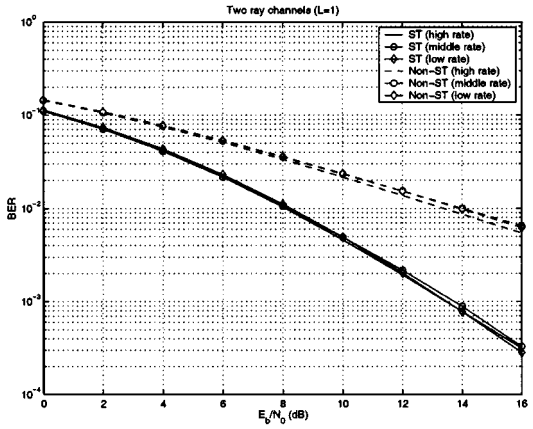

Fig. 3. Space-time gains $L = 1$.

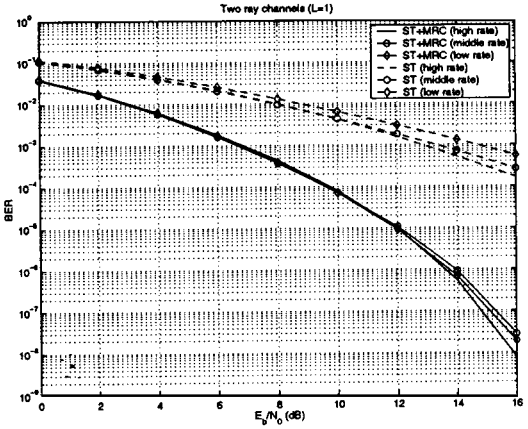

Fig. 5. MRC gains $L = 1$.

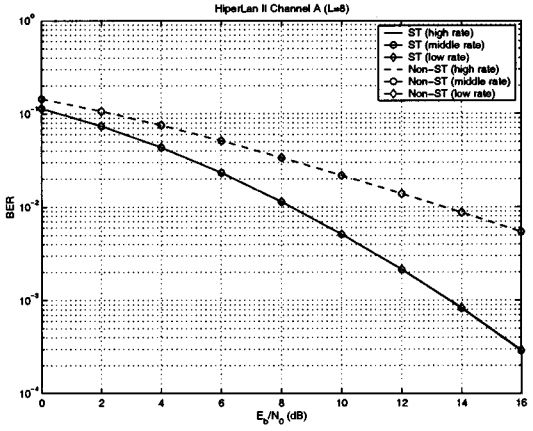

Fig. 4. Space-time gains HiperLan/2.

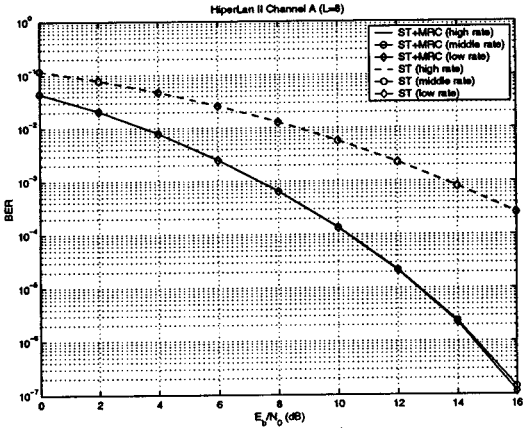

Fig. 6. MRC gains HiperLan/2.

assigned the weight $\phi_{lr} \approx 1/16$. In all simulations, the BER is chosen as the figure of merit and is averaged over 600 random channels and noise realizations for various E_b/N_0 points. Unless specified otherwise, the random channels $h_{mi}(l)$s are generated such that $h_{mi}(l)$s are independent for different m, i, and l. We generate the random channels based on two different channel models.

Two-Ray Channel $(L = 1)$*:* This corresponds to the case where the multipath consists of two equal-power dominant rays, and one ray is delayed with respect to the other by a chip duration.

HiperLan 2 Channel $(L = 8)$*:* The random channels are based on the HiperLan 2 channel model A, which corresponds to a typical office environment [4]. Each tap in the profile of channel model A is characterized by the Jakes' Doppler spectrum with a mobile speed of 3 m/s.

A. Single Receive Antenna

We compare our design with $N_t = 2$ transmit antennas and $N_r = 1$ receive antenna to that with a single transmit and receive antenna. The results are depicted in Figs. 3 and 4 for the aforementioned two channel models. Observing that the BER gains achieved by ST coding for all users is almost 5.8 dB at BER $= 10^{-2}$, it is deduced that our ST block-spreading code designs result in BER improvements even in the presence of frequency-selective FIR channels.

B. Two Receive Antennas

When the receiver has two antennas, there are two alternative paths we can follow to improve the overall system performance. The first (rather well-known) path is to retain the code assignments of Section II as if there was only one receive antenna and then employ maximum ratio combining (MRC) at each subcarrier to enhance the reliability of the symbol estimates. The second way is to apply subcarrier sharing techniques and then use two antennas to *double* system capacity in terms of either achievable transmission rates or maximum number of users, as we described in Section III.

Maximum Ratio Combining : Figs. 5 and 6 illustrate the performance improvement through MRC. It is observed that a savings in about 6 dB is obtained at BER $= 10^{-3}$, as compared with a single receive-antenna. Although it is well known that multiple receive antennas improve performance, this example indicates that array processing algorithms can be readily applied to our framework.

Doubling Network Capacity: We look at a system with a total of $2M$ users, who are divided into two identical groups with the same subcarrier allocations. In other words, each user in one group shares the same subcarriers with one in the other group. As described in Section III, two receive antennas can be used to separate two subcarrier-sharing users. We choose the linear two-stage ST receiver of Section III-B and compare it

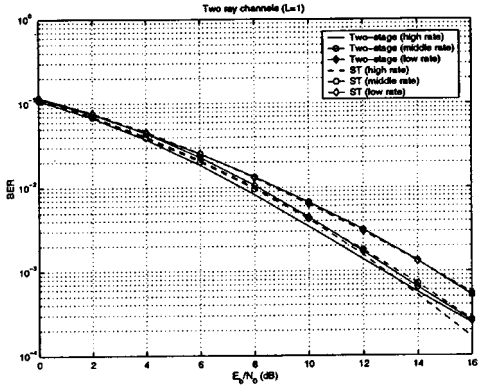

Fig. 7. Doubling network capacity $L = 1$.

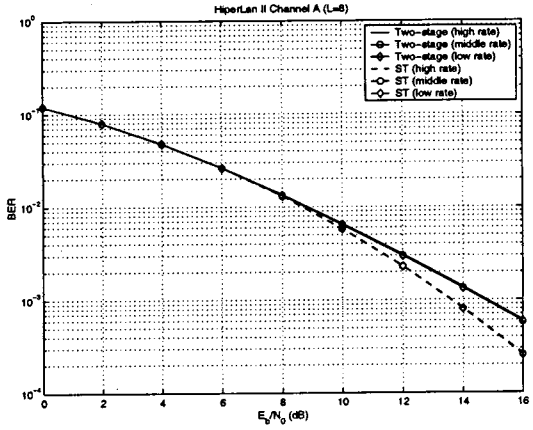

Fig. 8. Doubling network capacity HiperLan/2.

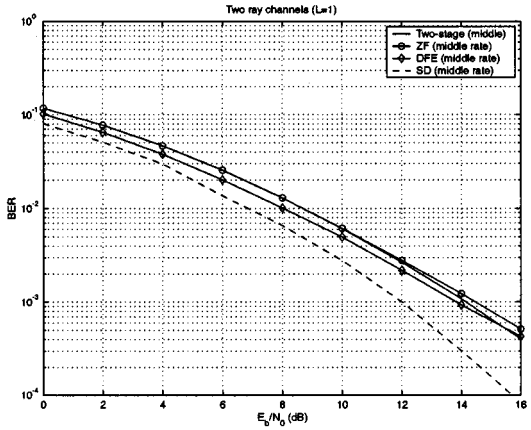

Fig. 9. Receiver comparison $L = 1$.

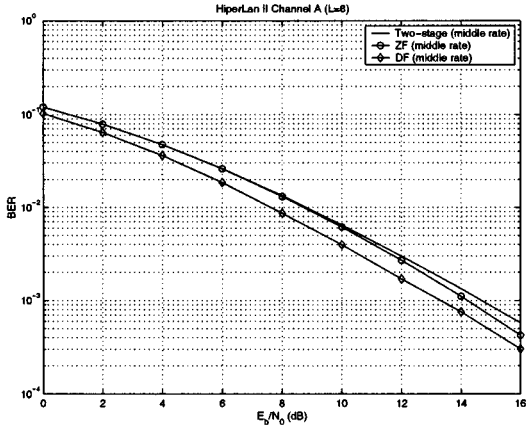

Fig. 10. Receiver comparison HiperLan/2.

with that of Section IV-A. As depicted in Figs. 7 and 8, we observe that systems with $2M$ users and two receive-antennas have (almost) the same BER performance as those with M users and one receive antenna. However, the system capacity in terms of the number of users is doubled with two receive antennas. Note also that instead of adding more users to the system, we could double the transmission rates of the existing users.

Comparison of Receivers: Finally, we compare the linear and DF receivers of Section III-A against the linear two-stage ST receiver of Section III-B and depict their respective performance in Figs. 9 and 10. Interestingly, the BER curves of these three receivers are very close. Intuitively speaking, the specific structure of the matrix $\mathbf{H}$ in (16) suggests that the condition number of $\mathbf{H}$ could be small. Thus, the linear receivers may not induce much noise enhancement. Although their BER performance is close, the two-stage ST receiver is better than the other two in terms of computational complexity.

We note that linear equalization of precoded transmissions is suboptimum. Although the maximum likelihood (ML) equalizer is expected to have superior performance, its high complexity (for linearly precoded transmissions) is prohibitive for high data rate transmissions. Consequently, to assess the performance penalty in a way similar to [27], we have applied the sphere decoder (SD)-based equalizer, and Fig. 9 depicts its BER performance. SD [24] achieves near ML performance with polynomial computational complexity (SD looks only at the precoded vectors that are "close" to a received symbol). Fig. 9 indicates that linear equalization imposes a penalty of about 2 dB at 10^{-3} bit error probability.

Effects of Channel Correlation: Thus far, the random channels $h_{mi}(l)$s are assumed to be independent for different m, i, and l. In order to investigate the effects of channel correlation on the BER performance, we randomly generate $h_{mi}(l)$s such that

$$E\left[h_{mi}(l)h^*_{m'i'}(l')\right] = \begin{cases} \frac{1}{L+1}, & \text{if } m = m', i = i', l = l' \\ \frac{\rho}{L+1}, & \text{otherwise} \end{cases}$$

where $E(\cdot)$ denotes expectation, and ρ controls the correlation between channels. We will use the two-ray channel model ($L = 1$). Fig. 11 shows the BER performance of the middle-rate user with correlated channels. It is observed that the channel correlation indeed imposes a small BER penalty on our designs.

We can conclude from these examples that without sacrificing the flexibility of our framework, adding a second receive antenna pays off either in terms of SNR or in terms of network capacity. Moreover, we can see how the more sophisticated receiver of Section III-B performs better.

V. Conclusions

In this paper, we have developed a multirate/multiuser OFDMA system that relies on ST coded block-spreaded transmissions. With a single receive antenna, our design guarantees

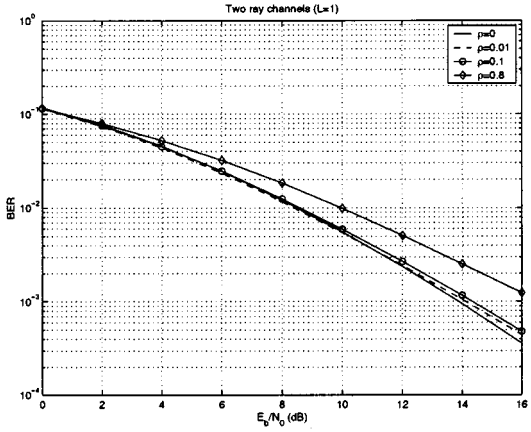

Fig. 11. BER with correlated channels.

deterministic symbol recovery with diversity gains regardless of the frequency-selective FIR channels and multiuser interference. Under favorable conditions (e.g., no frequency offset) with two receive antennas, our approach is capable of either improving BER performance or increasing (in terms of the number of users or supported transmission rates) the capacity of broadband wireless networks. Furthermore, the physical layer of our system facilitates multirate bandwidth allocation, which is an important feature in integrated services networks.

From a technical standpoint, our approach is based on a three-level user code design: The top level handles MUI, the middle level results in ST diversity gains, and the lower level mitigates ISI. Yet, the proposed framework is not computationally expensive, as it relies primarily on fast Fourier transform-based processing (and it could be implemented in a power-efficient way even on handheld receivers). As illustrated by simulations, the deterministic MUI elimination, ST diversity gains, and guaranteed symbol recovery (with a single receive antenna) lead to improved BER performance.

There are quite a few other approaches in our research agenda that could lead to further performance improvements. Acknowledging that the physical layer should be robust against channel fading and cope with time-varying channel conditions, the use of low-rate channel codes (such as the one half convolutional code) is a common practice in wireless transmissions. However, reliable channel estimation paired with beamforming (see, e.g., [22]), adaptive channel coding, and adaptive subcarrier allocation could provide opportunities for decreasing the overhead of channel encoding. Furthermore, it is in our plans to study whether it is possible to optimize our framework either in the deterministic sense (when channel status information is available at the transmitter) or in the stochastic sense (when only statistical description of the fading channels is known; see, e.g., [7]).

APPENDIX

Let us consider the set S of the all the $2J \times 2J$ matrices $\mathbf{S}$ with the special structure

$$\mathbf{S} = \begin{pmatrix} \mathbf{A} & \mathbf{B} \\ \mathbf{B}^* & -\mathbf{A}^* \end{pmatrix} \tag{23}$$

where $\mathbf{A}$ and $\mathbf{B}$ are $J \times J$ complex diagonal matrices. It is straightforward to verify that if $\mathbf{S}_1, \mathbf{S}_2 \in S$, then $\mathbf{S}_1 \pm \mathbf{S}_2 \in S$ as well. In a similar fashion, with $\mathbf{S}_3 \in S$, it holds that $\mathbf{S}_1\mathbf{S}_2\mathbf{S}_3 \in S$ (somewhat interestingly, it does not hold in general that $\mathbf{S}_1\mathbf{S}_2 \in S$). It also holds that for every $\mathbf{S} \in S$, the pseudoinverse $\mathbf{S}^\dagger$ also belongs to S. To see why, observe that the pseudoinverse $\mathbf{A}^\dagger$ of the upper left half of $\mathbf{S}$ is given by the diagonal matrix (see, e.g., [19, p. 448])

$$[\mathbf{A}^\dagger]_{k,k} = \begin{cases} 0, & :[\mathbf{A}]_{k,k} = 0 \\ ([\mathbf{A}]_{k,k})^{-1}, & :[\mathbf{A}]_{k,k} \neq 0, \end{cases} \quad 0 \leq k \leq J-1.$$

Recall that the Moore–Penrose pseudoinverse of $\mathbf{S}$ is defined as the unique matrix $\mathbf{S}^\dagger$, which satisfies the conditions (see, e.g., [16, p. 171])

$$\mathbf{S}\mathbf{S}^\dagger\mathbf{S} = f\mathbf{S}, \quad \mathbf{S}^\dagger\mathbf{S}\mathbf{S}^\dagger = \mathbf{S}^\dagger,$$
$$(\mathbf{S}\mathbf{S}^\dagger)^{\mathrm{T}} = (\mathbf{S}\mathbf{S}^\dagger), \quad (\mathbf{S}^\dagger\mathbf{S})^{\mathrm{T}} = (\mathbf{S}^\dagger\mathbf{S}).$$

As expected, if the matrix $\mathbf{S}$ is full rank, then $\mathbf{S}^\dagger = \mathbf{S}^{-1}$. It can be verified the aforementioned conditions are satisfied by

$$\mathbf{S}^\dagger := \begin{pmatrix} -(\mathbf{A}^*\mathbf{A} + \mathbf{B}^*\mathbf{B})^\dagger & \mathbf{0}_J \\ \mathbf{0}_J & -(\mathbf{A}^*\mathbf{A} + \mathbf{B}^*\mathbf{B})^\dagger \end{pmatrix} \cdot \begin{pmatrix} -\mathbf{A}^* & -\mathbf{B} \\ -\mathbf{B}^* & \mathbf{A} \end{pmatrix}$$

which belongs to S. As a result, if we look back to (15), (20a), and (20b), then it is clear that $\boldsymbol{H}_{1,1}, \boldsymbol{H}_{1,2}, \boldsymbol{H}_{2,1}, \boldsymbol{H}_{2,2} \in S$. Moreover, $\boldsymbol{H}_{1,1}^\dagger, \boldsymbol{H}_{2,2}^\dagger \in S$, and under the assumption of channel independence, $\boldsymbol{H}_{1,1}, \boldsymbol{H}_{2,2}$ are full rank. Hence, $\boldsymbol{H}_{1,1} - \boldsymbol{H}_{1,2}\boldsymbol{H}_{2,2}^{-1}\boldsymbol{H}_{2,1} \in S$, $\boldsymbol{H}_{2,2} - \boldsymbol{H}_{2,1}\boldsymbol{H}_{1,1}^{-1}\boldsymbol{H}_{1,2} \in S$, and the proof is complete.

REFERENCES

[1] D. Agrawal, V. Tarokh, A. Naguib, and N. Seshadri, "Space-time coded OFDM for high data-rate wireless communication over wideband channels," in *Proc. Veh. Technol. Conf.*, Ottawa, ON, Canada, May 18–21, 1998, pp. 2232–2236.

[2] S. M. Alamouti, "A simple transmit diversity technique for wireless communications," *IEEE J. Select. Areas Commun.*, vol. 16, pp. 1451–1458, Oct. 1998.

[3] "Broadband Radio Access Networks (BRAN); Hiperlan Type 2; Physical (PHY) layer," Eur. Telecommun. Stand. Inst., ETSI TS 101 475 v.1.1.1 (2000–04), 1998.

[4] "Channel Models for HIPERLAN/2 in Different Indoor Scenarios," Eur. Telecommun. Stand. Inst., Sophia-Antipolis, Valbonne, France, Norme ETSI, doc. 3ERI085B, 1998.

[5] G. J. Foschini and M. J. Gans, "On limits of wireless communication in a fading environment when using multiple antennas," *Wireless Pers. Commun.*, vol. 6, no. 3, pp. 311–335, Mar. 1998.

[6] G. B. Giannakis, Z. Wang, A. Scaglione, and S. Barbarossa, "AMOUR—Generalized multicarrier transceivers for blind CDMA irrespective of multipath," *IEEE Trans. Communications*, vol. 48, pp. 2064–2076, Dec. 2000.

[7] G. B. Giannakis and S. Zhou, "Optimal transmit-diversity precoders for random fading channels," in *Proc. GLOBECOM*, San Francisco, CA, Nov. 1, 2000, pp. 1839–1843.

[8] G. B. Giannakis, A. Stamoulis, Z. Wang, and P. Anghel, "Load-adaptive MUI/ISI-resilient generalized multi-carrier with linear and DF receivers," *Eur. Telecommun. Trans.*, vol. 11, no. 6, pp. 527–537, Nov./Dec. 2000.

[9] M. L. Honig and J. B. Kim, "Allocation of DS-CDMA parameters to achieve multiple rates and qualities of service," in *Proc. GLOBECOM*, vol. 3, New York, 1996, pp. 1974–1978.

[10] Z. Liu and G. B. Giannakis, "Space-time block-coded multiple access through frequency-selective fading channels," *IEEE Trans. Commun.*, vol. 49, pp. 1033–1044, June 2001.
[11] Z. Liu, G. B. Giannakis, B. Muquet, and S. Zhou, "Space-time coding for broadband wireless communications," *Wireless Commun. Mobile Comput.*, vol. 1, no. 1, pp. 33–53, Jan.–Mar. 2001.
[12] A. F. Naguib, N. Seshadri, and R. Calderbank, "Space-time coding and signal processing for high data rate wireless communications," *IEEE Signal Processing Mag.*, vol. 17, pp. 76–92, May 2000.
[13] A. K. Parekh and R. G. Gallager, "A generalized processor sharing approach to flow control in integrated service network," *IEEE/ACM Trans. Networking*, vol. 1, pp. 344–357, June 1993.
[14] T. S. Rappaport, *Wireless Communications: Principles and Practice*. Englewood Cliffs, NJ: Prentice-Hall, 1996.
[15] A. Scaglione, G. B. Giannakis, and S. Barbarossa, "Redundant filterbank precoders and equalizers part I: Unification and optimal designs," *IEEE Trans. Signal Processing*, vol. 47, pp. 1988–2006, July 1999.
[16] J. R. Schott, *Matrix Analysis for Statistics*. New York: Wiley, 1997.
[17] A. Stamoulis and G. B. Giannakis, "Packet fair queueing scheduling based on multirate multipath-transparent CDMA for wireless networks," in *Proc. INFOCOM*, Tel Aviv, Israel, Mar. 2000, pp. 1067–1076.
[18] A. Stamoulis, G. B. Giannakis, and A. Scaglione, "Block FIR decision-feedback equalizers for filterbank precoded transmissions with blind channel estimation capabilities," *IEEE Trans. Commun.*, vol. 49, pp. 69–83, Jan. 2001.
[19] G. Strang, *Linear Algebra and its applications*, 3rd ed. Orlando, FL: Harcourt Brace Jovanovich, 1988.
[20] T. Ottosson and A. Svensson, "On schemes for multirate support in DS/CMDA," *Wireless Pers. Commun.*, vol. 6, no. 3, pp. 265–287, Mar. 1998.
[21] V. Tarokh, A. Naguib, N. Seshadri, and A. R. Calderbank, "Combined array processing and space-time coding," *IEEE Trans. Inform. Theory*, vol. 45, pp. 1121–1128, May 1999.
[22] A. J. Van Der Veen, "Algebraic methods for deterministic blind beamforming," *Proc. IEEE*, vol. 86, pp. 1987–2008, Oct. 1998.
[23] A. J. Viterbi, *CDMA Principles of Spread Spectrum Communication*. Reading, MA: Addison-Wesley, 1995.
[24] E. Viterbo and J. Bouros, "A universal lattice code decoder for fading channels," *IEEE Trans. Inform. Theory*, vol. 45, pp. 1639–1642, July 1999.
[25] Z. Wang and G. B. Giannakis, "Block spreading for multipath-resilient generalized multi-carrier CDMA," in *Signal Processing Advances in Wireless Communications*, G. B. Giannakis, P. Stoica, Y. Hua, and L. Tong, Eds. Englewood Cliffs, NJ: Prentice-Hall, 2000, vol. II.
[26] ——, "Wireless multicarrier communications: Where Fourier meets Shannon," *IEEE Signal Processing Mag.*, vol. 17, pp. 29–48, May 2000.
[27] ——, "Linearly precoded or coded OFDM against wireles channel fades?," in *Proc. 3rd IEEE Workshop Signal Process. Advances Wireless Commun.*, Taoyuan, Taiwan, R.O.C., Mar. 20–23, 2001, pp. 267–270.

Anastasios Stamoulis received the the Diploma degree in computer engineering from University of Patras, Patras, Greece, in 1995, the M.Sc. degree in computer science from the University of Virginia, Charlottesville, in 1997, and the Ph.D. degree in electrical engineering from the University of Minnesota, Minneapolis, in 2000.

He joined the AT&T Shannon Laboratory, Florham Park, NJ, as a Senior Technical Staff Member in 2001.

Zhiqiang Liu received the B.S. degree from the Department of Radio and Electronics, Peking University, Beijing, China, in 1991, the M.E. degree from the Institute of Electronics, Chinese Academy of Science, Beijing, in 1994, and the Ph.D. degree from the Department of Electrical and Computer Engineering, University of Minnesota, Minneapolis, in 2001.

From 1995 to 1997, he worked as a research scholar at the Department of Electrical Engineering, National University of Singapore. From 1999 to 2001, he was a research assistant with the University of Minnesota. He is now an assistant professor with the Department of Electrical and Computer Engineering, University of Iowa, Iowa City. His research interests lie in the areas of wireless communications and signal processing, including space-time coding, wideband wireless communication systems, multiuser detection, and multicarrier and blind channel estimation algorithms.

Georgios B. Giannakis (F'97) received the Dipl.Eng. degree in electrical engineering from the National Technical University of Athens, Athens, Greece, in 1981. From September 1982 to July 1986, he was with the University of Southern California (USC), Los Angeles, where he received the M.Sc. degree in electrical engineering in 1983, the M.Sc. degree in mathematics in 1986, and the Ph.D. degree in electrical engineering in 1986.

After lecturing for one year at USC, he joined the University of Virginia, Charlottesville, in 1987, where he became a Professor of Electrical Engineering in 1997. Since 1999, he has been a Professor with the University of Minnesota, Minneapolis, where he now hold an ADC Chair in wireless telecommunications. His general interests span the areas of communications and signal processing, estimation and detection theory, time-series analysis, and system identification, subjects on which he has published more than 130 journal papers, 270 conference papers, and two edited books. Current research topics focus on transmitter and receiver diversity techniques for single- and multiuser fading communication channels, redundant precoding and space-time coding for block transmissions, and multicarrier and wideband wireless communication systems. He is a frequent consultant to the telecommunications industry.

Dr. Giannakis was the (co-) recipient of best paper awards from the IEEE Signal Processing (SP) Society in 1992, 1998, and 2000. He also received the Society's Technical Achievement Award in 2000. He co-organized the IEEE-SP Workshops on HOS in 1993, SSAP in 1996, and SPAWC in 1997 and guest (co-) edited four special issues. He has served as an Associate Editor for the IEEE TRANSACTIONS ON SIGNAL PROCESSING and the the IEEE SIGNAL PROCESSING LETTERS, a secretary of the SP Conference Board, a member of the SP Publications Board, and a member and vice chair of the Statistical Signal and Array Processing Committee. He is a member of the Editorial Board for the PROCEEDINGS OF THE IEEE, he chairs the SP for Communications Technical Committee, and serves as the Editor in Chief for the IEEE SIGNAL PROCESSING LETTERS. He is a member of the IEEE Fellows Election Committee and the IEEE-SP Society's Board of Governors.